CHARACTERIZATION OF HIDDEN AIRFRAME CORROSION BY TIME-RESOLVED INFRARED RADIOMETRY (TRIR)

J. W. M. Spicer, W. D. Kerns, L. C. Aamodt, and J. C. Murphy
Center for NDE AND Applied Physics Laboratory
The Johns Hopkins University
Johns Hopkins Road, Laurel, MD 20723-6099, USA

INTRODUCTION

Since hidden corrosion is expected to be the primary factor limiting the service life of military and civilian aircraft, the problem of detection of hidden corrosion needs to be solved to allow for life extension. A quantitative thermographic NDE technique for the characterization of hidden corrosion is under development along with supporting theoretical analysis. In earlier work [1,2] we have shown that the technique of time-resolved infrared radiometry (TRIR) is an effective method for quantitatively detecting coating thickness variations and for characterizing the degree of coating disbonding in terms of equivalent air gaps. In this paper we examine the applicability of TRIR techniques to the characterization of corrosion damage in airframes by investigating plate specimens of 2024-T3 aluminum with both milled defects and corroded regions produced by an accelerated corrosion test.

The TRIR technique is a thermal characterization method which has some distinct differences from other pulsed thermography techniques. The time development of the surface temperature is monitored as a function of time as a heating pulse is applied to the specimen as indicated in the schematic diagram in Fig. 1. Advantages of this approach are that the depth of the defect and its thermal characteristics are easily determined with only one measurement without the need for a calibration measurement made on a defect-free region of the specimen. Also, since it is the shape of the temperature-time curve and not its absolute magnitude which provides the quantitative information about the defects, the technique can be self-calibrating for variations in emissivity and optical absorption. Finally, since heat is continuously applied to the specimen at a low power, the temperature rise produced with this method need never be more than a few degrees. This is in contrast to flash techniques which deposit a lot of energy in the sample in a short pulse which can produce very high temperature excursions at the beginning of the measurement, sometimes sufficiently large to damage the sample.

Quantitative information on the thermal characteristics of a subsurface structure are obtained from analysis of the TRIR temperature-time curves which display the surface temperature at a point on the sample as a function of the square root of time. These curves are a necessary companion to the full-field images of surface temperature. Loss of material due to corrosion creates a variation in the skin thickness which will be identified by a variation in the thermal transit time through the skin. The presence of corrosion product will be identifiable through a variation in the heat flow at the underside of the skin and will provide a variation in the slope of the temperature-time curve after the thermal transit time.

Review of Progress in Quantitative Nondestructive Evaluation, Vol. 12
Edited by D.O. Thompson and D.E. Chimenti, Plenum Press, New York, 1993

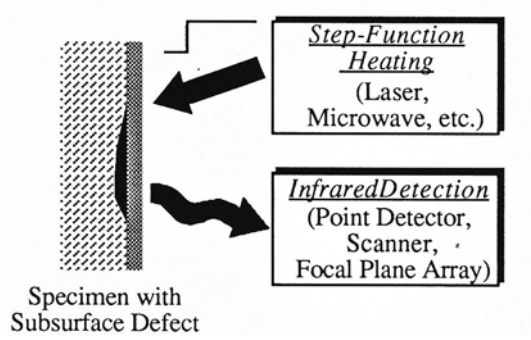

Fig. 1. Schematic diagram describing the time-resolved infrared radiometry technique.

The next section presents some theoretical calculations of the TRIR response expected for a series of experimental situations. These include examining the effect of varying the thickness of the corrosion product, varying the skin thickness and varying the area of the heating source. Then TRIR measurements will be reported for milled defects of different depths to demonstrate the sensitivity of the technique for measuring different skin thicknesses. A series of milled slots of different separations are then imaged to show the capability for resolving the lateral extent of defect regions. The thermal structure of a region of corrosion is then studied directly with the TRIR technique in order to understand the effect of the corrosion on thermal transport through the structure. TRIR studies of various multilayer configurations of aluminum plates with and without corroded regions and adhesives are presented to replicate the case of identifying corrosion in a lap joint. One of the main goals in this work is to separate the thermal signal due to metal loss in 1st and lower layers from the thermal signal due to the presence of corrosion product, particularly when adhesives and sealants are present.

MODELLING OF EXPECTED TRIR RESPONSES

A series of calculations were made using a one-dimensional multilayer theoretical model [3] in order to determine the range of TRIR temperature-time responses expected for a multilayer aluminum system with a varying amount of corrosion product present beneath the skin. The system considered is shown in Fig. 2 and consisted of a 1.6 mm thick sheet of 2024-T3 aluminum on a 2024-T3 aluminum substrate with five different thicknesses of corrosion product as an intervening layer. This represents the case of corrosion on the underside of the top skin layer with intimate contact to the next layer of aluminum below as occurs at a lap joint or at a stringer. The one-dimensional nature of the model implies that the heating source is uniformly distributed over the entire sample surface and that only thermal structures which are parallel to the sample surface are considered.

The results of the calculations are shown in Fig. 2 along with a reference curve which is the TRIR response for a thermally thick specimen of 2024-T3. The reference curve is the response expected when there is no corrosion product present. All of the temperature-time curves are plotted as a function of the square root of time since the reference curve shows a linear dependence in such a plot. Comparison of the reference curve with the curves obtained for different corrosion product thicknesses reveals that all of the curves follow the same straight line until almost 0.2 $sec^{1/2}$. This is the thermal transit time, the time at which the interface between the top skin layer and the corrosion product is detected. This time is given by $0.38\ L^2/\alpha$ where L is the thickness of the layer and α is the thermal diffusivity of the layer.

The top curve in Fig. 2 shows the response for a corrosion product layer of thickness 1 mm. Here the slope of the curve increases after the thermal transit time of the 1.6 mm layer

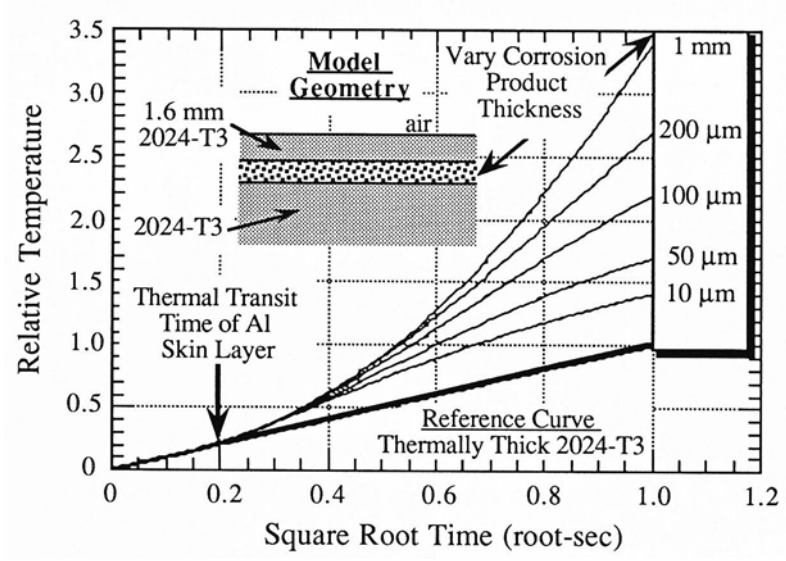

Fig. 2. Calculated temperature-time curves using a multilayer model showing the effect on the TRIR response of varying the thickness of the corrosion product beneath a 1.6 mm thick skin of 2024-T3 aluminum .

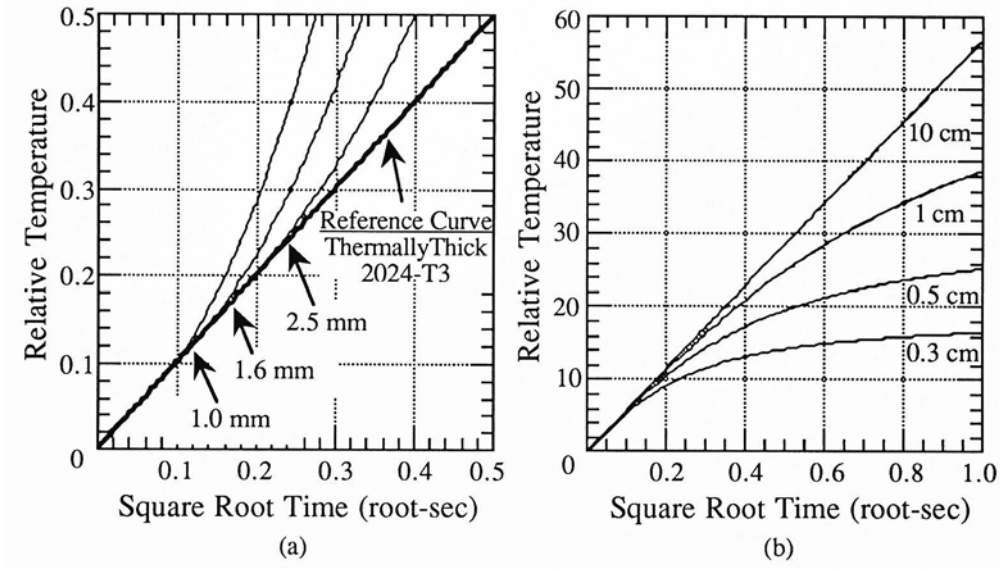

Fig. 3. (a) Calculated temperature-time curves using a one-dimensional model for different thicknesses of 2024-T3 aluminum showing the increase in thermal transit time with skin thickness. (b) Calculated temperature-time curves using a three-dimensional model for a thermally-thick specimen of 2024-T3 aluminum showing the effect of lateral heat flow on the TRIR response.

due to the thermally insulating nature of the corrosion product. As the thickness of the corrosion product is decreased, a range of responses is obtained which approach the reference curve for a very thin layer of corrosion product. These curves show that, for this one-dimensional model, the TRIR technique will be sensitive to the presence of corrosion product beneath an aluminum skin. In addition, the shape of the TRIR response curve is a function of the thickness of the corrosion layer.

Since the thermal transit time depends on the layer thickness as described above, variations in the thickness of the aluminum skin can be monitored by measurement of the thermal transit time. This is demonstrated in the theory curves shown in Fig. 3(a) which gives the TRIR temperature-time curves for aluminum skins of thicknesses 1.0, 1.6 and 2.5 mm. The arrows indicate the thermal transit time for each thickness and it is clear that this time increases with increasing skin thickness. These curves are again calculated using a one-dimensional model.

When a material with a high thermal diffusivity such as aluminum is heated with a laser source with finite lateral extent, lateral heat flow in the plane of the sample is expected to be observed. This effect is examined in Fig. 3(b). Here the TRIR response is shown for a thermally-thick specimen of 2024-T3 aluminum for heating beam radii of 0.3, 0.5, 1 and 10 cm. The 10 cm heating beam satisfies the case for one-dimensional heating over the time range of 1 sec since the response follows the expected straight line when plotted as a function of the square root of time as was seen in the reference curves of Figs. 2 and 3(a). As the heating beam radius is decreased, however, lateral heat flow effects become more pronounced and are evident as a decreasing slope in the TRIR response curve. These effects will be observed in the experimental results reported in the next section since a focussed laser source was used in order to obtain a sufficient temperature rise for detection with the infrared system. It is still possible, however, to see the effect of varying thermal transit times and varying thermal mismatch at the bottom surface of the skin layer in these measurements once account has been taken of the effects of the lateral heat flow.

EXPERIMENTAL RESULTS

In the TRIR measurements to be discussed here, an argon laser was used as the heating source. Some preliminary experiments have been conducted using induction heating, but these will not be reported here. The IR detection system used is an infrared scanner which provides continuous monitoring of surface temperature along a single line. With this system a time resolution of 8.3 msec for the development of surface temperature can be achieved. We have also introduced an InSb focal plane array into our experimental setup and this provides a greater sensitivity, greater time resolution and the capability of simultaneously monitoring a full field area on the specimen.

Specimens with Milled Defects

In order to simulate loss of skin thickness, we have prepared specimens with milled defects of known depth and lateral extent in plates of 2024-T3 aluminum. The purpose of these specimens is to provide test specimens with well-known defect sizes in order to calibrate the results of the TRIR measurements. Figure 4 shows the TRIR responses obtained for three different aluminum skin thicknesses. Note that while each of these curves shows the general shape indicative of lateral heat flow discussed in Fig. 3(b), it is possible to identify different thermal transit times for the different thicknesses. The thermal transit times indicated in Fig. 4 for the 1.3 mm and 2.4 mm thick layers are those calculated using a handbook value for the thermal diffusivity of 2024-T3 aluminum. These calculated transit times show good agreement with the experimental transit times evident in the data.

The next specimen considered is shown in Fig. 5 and consisted of 4 slots of uniform depth milled with varying separations. A contour representation of a TRIR X-Y image after

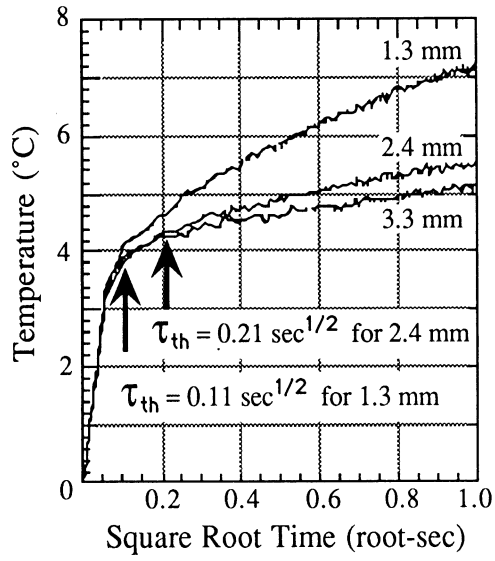

Fig. 4. Experimental temperature-time curves for different thicknesses of 2024-T3 aluminum. The transit times expected from theory are indicated by the arrows.

1 second of heating is also shown in Fig. 5 and shows that the four subsurface slots have been detected. Further analysis of this image is provided in Fig. 6(a) which compares the temperature-time response for intact material with the response for a region over slot C. The thermal transit time down to the slot is clearly evident and the location over the slot shows greater slope values than the region of intact material. The variation in surface temperature as a function of position across the slots is shown in Fig. 6(b). The position and extent of the slots are also indicated in the figure and show that the TRIR image has accurately identified the positions of the slots.

Specimens from an Accelerated Corrosion Test

Laboratory corrosion specimens were produced by following ASTM G34-90 "Standard Test Method for Exfoliation Corrosion Susceptibility in 2XXX and 7XXX Series Aluminum Alloys" on plates of 2024-T3 aluminum of varying thicknesses. We have produced a range in severity of corrosion by varying the time of exposure of the plates to a solution of NaCl, KNO_3 and HNO_3.

Initial TRIR measurements were performed directly on the corroded surfaces to establish the types of thermal responses provided by the presence of the corrosion. It was expected that exfoliation corrosion would produce significant thermal contrast due to the development of a stratified structure in the aluminum with corrosion product present in the layers. This causes significant surface morphology changes with localized mounds and pits. It was confirmed that this stratified structure was generated by our exfoliation test by cross-sectioning a sample after 210 hours of exposure. A selection of the TRIR curves obtained on this sample are given in Fig. 7. Curves C and D were obtained at from regions with minimal corrosion and resemble the TRIR response for intact material shown in Fig. 6(a). Curves C and D were obtained at corroded regions exhibiting dramatic surface morphology changes and show a much stronger temperature rise indicating poor thermal conduction into the aluminum specimen due to the presence of the subsurface structure with air gaps and corrosion product. These curves indicate that there should be sufficient thermal contrast at a corroded surface to enable detection of this corrosion beneath a covering skin layer.

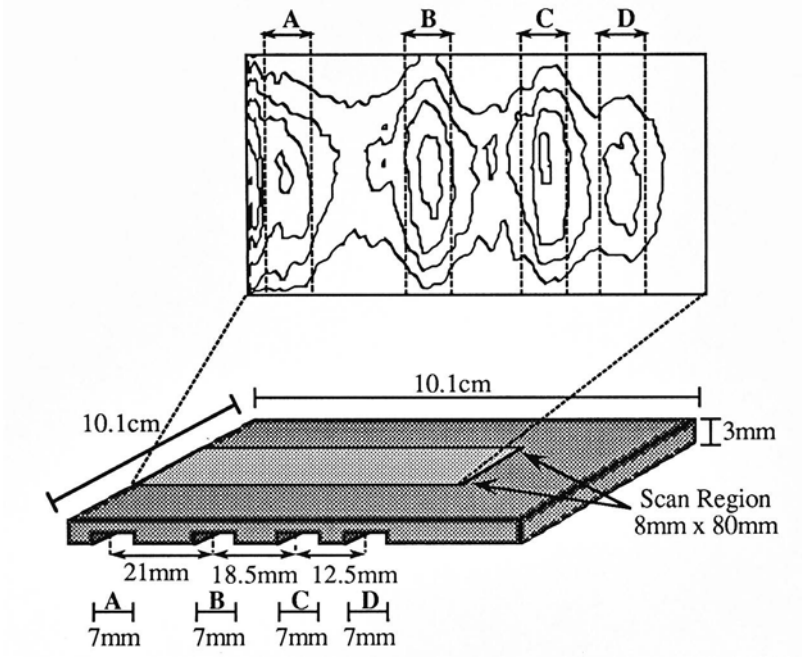

Fig. 5. Contour representation of TRIR X-Y scan performed on 2024-T3 aluminum specimen with 7 mm wide slots milled with differing separations. Highest response in the contour image is over the slots.

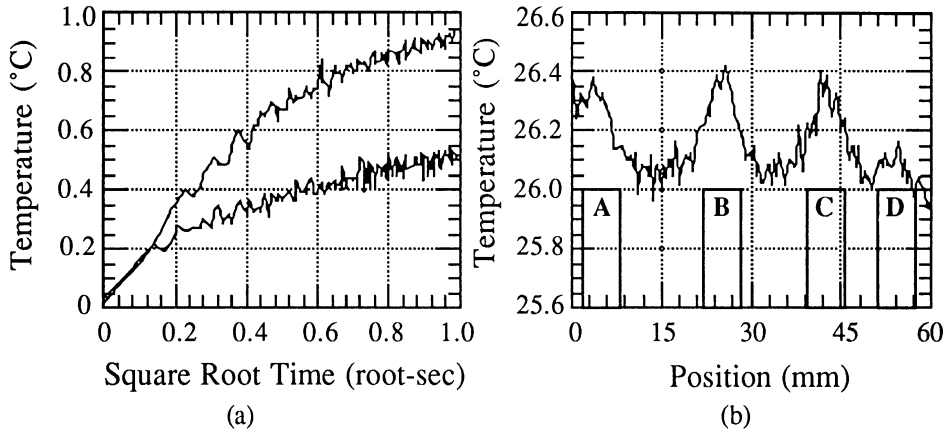

Fig. 6. (a) Analysis of TRIR X-Y image data in Fig. 5 showing temperature-time curves for location over slot C and for a location without slot. (b) Plot of temperature vs. position along a line over the slots. The locations of the slots are indicated at the bottom of the graph.

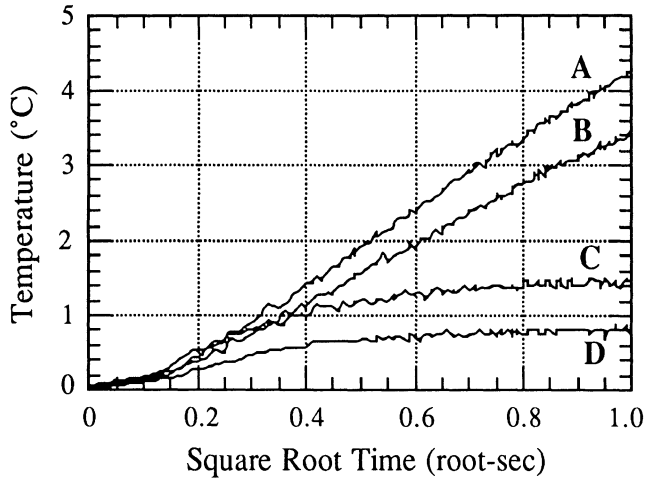

Fig. 7. TRIR temperature-time curves performed directly on corroded regions in 2024-T3 aluminum. Curves A and B were acquired at locations with severe surface morphology changes. Curves C and D are from locations of less severe corrosion.

A test specimen was then constructed to investigate the detectability of second layer corrosion beneath a top layer with an adhesive present. An aluminum plate of thickness 1.6 mm was bonded using a thermally-conductive adhesive to a specimen which had been corroded over half of its surface. TRIR response curves obtained for positions on the top layer over both corroded and uncorroded regions are shown in Fig. 8. These TRIR responses show that the expected thermal transit time of 0.14 $sec^{1/2}$ for the top plate is evident in the experimental data and that the TRIR response for the position over the corroded material shows a higher temperature response than that over the intact material. This is in agreement with the theoretical curves shown in Fig. 2 when the lateral heat flow effects described in Fig. 3(b) are taken into account.

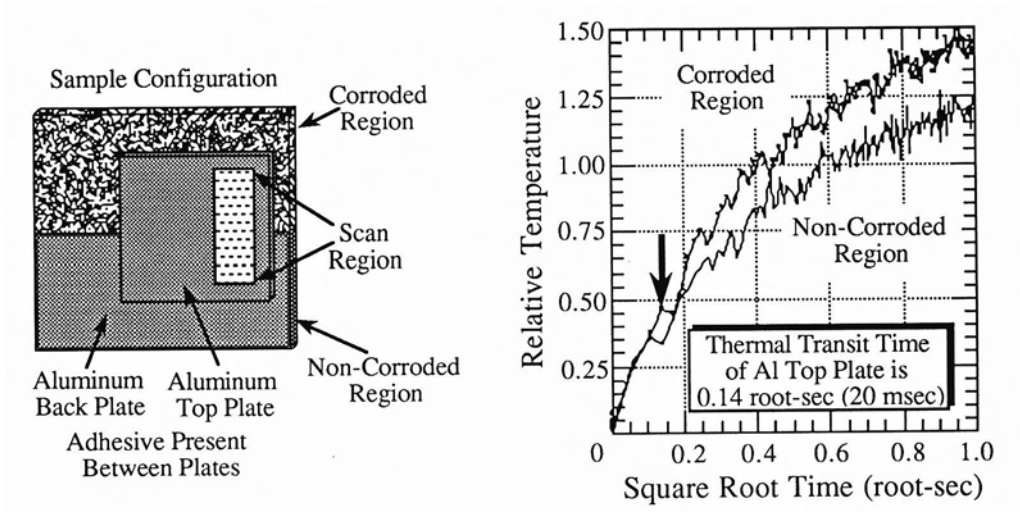

Fig. 8. TRIR temperature-time curves showing detection of corrosion product beneath top plate of thickness 1.6 mm.

CONCLUSIONS

The TRIR method has been shown to have strong potential for the characterization of hidden airframe corrosion. Experiments on specimens with milled defects have shown that the TRIR method can image extent of subsurface loss of skin thickness and that the amount of remaining skin thickness can be calculated from the thermal transit time. It has also been shown that the presence of corrosion product in 2024-T3 Al provides sufficient thermal effusivity mismatch for detection by TRIR and that second layer corrosion can be detected when a sealant material is present at the lap joint.

ACKNOWLEDGEMENTS

This work was sponsored by the Center for Advanced Nondestructive Evaluation, operated by the Ames Laboratory, USDOE, for the Air Force Wright Laboratory/Materials Directorate under Contract No. W-7405-ENG-82 with Iowa State University and by the U.S. Department of the Navy under Contract N00038-89-C-5301.

REFERENCES

1. J.W. Maclachlan Spicer, W.D. Kerns, L.C. Aamodt and J.C. Murphy, J. Nondestructr. Eval. 8, No. 2, 107-120 (1989).
2. J.W. Maclachlan Spicer, W.D. Kerns, L.C. Aamodt and J.C. Murphy, in Review of Progress in Quantitative NDE, edited by D.O. Thompson and D.E. Chimenti (Plenum Press, New York, 1991) Vol. 10, pp. 1193-1200.
3. L.C. Aamodt, J.W. Maclachlan Spicer and J.C. Murphy, J. Appl. Phys. 68, No. 12, 6087-6098 (1990).